〈Original Article〉

Structural prediction and interpretation of the substrate specificity of a lactate oxidase from *Enterococcus* sp. NBRC3427

Misaki Hiruta[1] and Yoshiaki Nishiya[1]

Summary Lactate oxidase (Lox) is utilized in clinical lactate assays and lactate biosensors. Lox from *Enterococcus* sp. NBRC3427 (LoxL) is considered suitable for use in applications. For predicting the enzyme's substrate specificity, the tertiary structure of LoxL was constructed using homology modeling based on the X-ray crystal structure of Lox from *Aerococcus viridans*, which exhibited approximately 52% homology with LoxL. The LoxL structure model was used for docking simulations between LoxL and L-lactate, L-mandelate, L-glycerate, and L-phenyllactate, which revealed marked steric interference between LoxL and L-mandelate. The gene encoding LoxL with a C-terminal His-tag was expressed in *Escherichia coli*, and LoxL was purified to homogeneity. The specific activities of LoxL for L-mandelate, DL-glycerate, and L-phenyllactate were 6.6×10^{-5}, 6.6×10^{-3}, and 9.6×10^{-3} of the L-lactate value, respectively. These results accorded with the interpretation based on the structural prediction and could aid efforts to improve the enzyme's substrate selectivity using protein engineering techniques.

Key words: Lactate oxidase, *Enterococcus*, Structural model, Substrate docking, Substrate specificity

1. Introduction

Lactate oxidase (Lox, EC 1.1.3.2) is a homotetrameric flavoprotein containing one flavin mononucleotide (FMN) per subunit as a coenzyme. Lox catalyzes the following reaction[1]:

L-lactate + O_2 → pyruvate + H_2O_2

The lactate concentration in the blood rises with fatigue during exercise and acts as a stress indicator as well as an indicator of diseases such as lactic acidosis[2]. The enzyme LoxL (Lox from *Enterococcus* sp. NBRC3427, formerly *Lactococcus lactis* subsp. *cremoris* IFO3427) has been used in clinical diagnostic reagents and biosensors for the measurement of lactate[1]. However, the enzymatic properties of LoxL remain poorly understood because the three-dimensional structure of the enzyme has yet to be elucidated.

This report describes a three-dimensional

[1]Department of Life Science, Setsunan University, 17-8 Ikeda-Nakamachi, Neyagawa, Osaka 572-8508, Japan.

To whom correspondence should be addressed.
Dr. Yoshiaki Nishiya
Department of Life Science, Setsunan University, 17-8 Ikeda-Nakamachi, Neyagawa, Osaka 572-8508, Japan.
E-mail: nishiya@lif.setsunan.ac.jp,
Fax: +81-72-838-6599

Received for publication April 24, 2017
Accepted for publication May 10, 2017

structure of LoxL modeled on the basis of its homology to Lox from *Aerococcus viridans* (LoxA)[3]. LoxA has been thoroughly studied using X-ray crystallography, and the substrate binding features of possible importance as well as the enzyme's catalytic mechanism have been reported[4-7]. The structure model of LoxL described here provides a reasonable starting point for determining structure-function relationships.

In this study, the substrate specificity of LoxL was also structurally predicted using docking simulations between the LoxL structure model and compounds bulkier than L-lactate, such as L-mandelate, L-glycerate, and L-phenyllactate. Optical isomers of these compounds are used as pharmaceutical raw materials and have potential applications in food preservation. The substrate specificity of purified LoxL determined here supports interpretations based on the structural prediction. These data could aid efforts to improve the enzyme's substrate selectivity using protein engineering techniques.

2. Materials and Methods

Materials

Compounds and reagents were purchased from Nacalai Tesque (Kyoto, Japan) or Wako Pure Chemical Industries (Osaka, Japan).

Sequence homology analysis

Amino acid sequence homologies were analyzed using ClustalW2 (http://www.ebi.ac.uk/Tools/clustalw2/)[8] and GENETYX software (Software Development Co., Ltd., Tokyo, Japan). The amino acid sequences of LoxL and LoxA (DDBJ accession numbers J6Y8E1 and Q44467, respectively) were aligned to determine sequence identities and conserved sequences.

Homology modeling and docking simulations

Homology modeling was used to build the LoxL model. MODELLER[9] software was used to generate a three-dimensional protein model based on the structure of LoxA (PDB ID: 2e77b). Energy minimization was applied to the model to further refine the structure. There was only one outlier on the Ramachandran plot of the model. This outlier, identified as residue S293, was found to be far from the active site (>10 Å).

MOE (Chemical Computing Group Inc., Montreal, Canada)[10] and Pymol[9] software were used for molecular visualization and docking simulations. A model of the LoxL binding site containing pyruvate and FMN was obtained by superposing the coordinates of the LoxL active site onto those of LoxA bound to both ligands. The coordinates for various compounds were then generated by superposing the positions of the carboxylate and hydroxyl groups onto those of the carboxylate and ketone groups of pyruvate. Molecular structures of compounds used in the docking simulations were obtained from the PubChem database (https://pubchem.ncbi.nlm.nih.gov/).

Bacterial strains, plasmid, and culture conditions

Escherichia coli strains DH5α and BL21(DE3) and the plasmid pET29a (Km^r) were used for recombinant strain preparation and plasmid construction, respectively. Bacteria were grown in LB broth or on LB agar (LB broth plus 1.5% agar) at 30°C. The antibiotic used was kanamycin (30 μg/mL).

General DNA manipulation

Plasmid isolation, cleavage of DNA with restriction enzymes, and ligation of DNA with T4 DNA ligase were carried out as described previously[10,11]. Transformation of *E. coli* was carried out according to the competent-cell method[12]. A KOD-Plus Mutagenesis kit (Toyobo Co., Ltd., Osaka, Japan) was used for constructing the gene encoding LoxL with a C-terminal His-tag. Polymerase chain reaction (PCR) was performed according to manufacturer's instruction.

Recombinant plasmid construction

The gene encoding LoxL was artificially synthesized by the manufacturer (Life Technologies, Foster City, CA, USA). The codon usage was adapted to the codon bias of *E. coli* genes. In

addition, regions of very high (>80%) or very low (<30%) GC content were avoided where possible. The 1,113-bp synthesized DNA was ligated between the *Nde*I and *Bam*HI sites of pET29a, and the recombinant construct was designated pET-Lox. An additional His-tag sequence was then introduced into the C-terminus of LoxL by inverse PCR using the mutagenesis kit and the following primers: 5'-GGATCCAAGCTTGCGGCCGCACTCGAGCA-3' (sense primer, corresponding to the sequence that encodes the 6×His-tag plus spacer peptide GSKLAAALEHHHHHH and the stop codon) and 5'-GATGAAGCGGTTCTCGCGCAGTTTGAT-3' (antisense primer, complementary to the sequence that encodes the C-terminal peptide IKLRENRFI). This construct was designated pET-LoxHT. The DNA sequences of the constructs were verified by sequencing. The pET-Lox and pET-LoxHT carriers were induced to synthesize the gene product by the addition of isopropyl-L-D-thiogalactopyranoside (IPTG) to the culture medium.

Enzyme purification

E. coli BL21(DE3)(pET-LoxHT) was grown in LB medium (400 mL) containing 30 μg/mL of kanamycin at 30°C for 2.5 h with rotation at 100 rpm. The culture was then supplemented with 0.1 mmol/L IPTG and 5% glycerol, and the cells were cultured for an additional 7 h at 30°C to stationary phase. The cells were harvested by centrifugation and re-suspended in 20 mmol/L potassium phosphate buffer (pH 7.5). A crude extract was prepared by sonication of the cells following centrifugation. The supernatant was then loaded onto a His GraviTrap immobilized metal affinity chromatography column (GE Healthcare, Uppsala, Sweden). LoxL was eluted using 20 mmol/L potassium phosphate buffer (pH 7.5) containing 200 mmol/L imidazole, 500 mmol/L NaCl, 1% Triton X-100, and 20% glycerol. Pooled fractions exhibiting Lox activity were finally purified to homogeneity by gel filtration with a HiTrap Desalting column (GE Healthcare) using 20 mmol/L potassium phosphate (pH 7.5) for elution. The enzymatic properties of the purified product were then characterized.

Enzyme assay and characterization

The enzyme assay was based on the measurement of hydrogen peroxide produced during substrate oxidation. A 4-aminoantipyrine peroxidase system was used for the enzyme assay, as described previously[1]. The final assay mixture contained 25 mmol/L L-lactate (half of this concentration for L-mandelate, DL-glycerate, and L-phenyllactate), 1.2 mmol/L 4-aminoantipyrine, 0.76 mmol/L N-ethyl-N-(2-hydroxy-3-sulfopropyl)-3-methylaniline (TOOS), 20 mmol/L potassium phosphate buffer (pH 7.5), and 2.4 U/mL of horseradish peroxidase. Enzyme solution (50 μL) was incubated with the assay mixture (1,000 μL) at 37°C, and the amount of quinoneimine dye formed by the coupling of 4-aminoantipyrine, TOOS, and horseradish peroxidase was measured spectrophotometrically at 555 nm against a sample blank. One unit of activity was defined as the formation of 1 μmol of hydrogen peroxide (0.5 μmol of quinoneimine dye) per minute at 37°C and pH 7.5. Reaction mixtures consisting of various concentrations of substrate solution were used to determine the K_m value. Molecular weight was determined by sodium dodecyl sulfate–polyacrylamide gel electrophoresis (SDS-PAGE)[1].

3. Results and Discussion

Molecular modeling of LoxL

As shown in Figure 1, LoxL exhibited a relatively high degree of homology with LoxA (estimated at 52.1% identity). Except for the termini, only 2 alignment gaps, consisting of 1 and 2 residues, respectively, were observed. The active site of LoxA was composed of 8 residues: Y40, A95, Y146, D174, R181, K241, H265, and R2686. These residues correspond to LoxL residues Y37, A92, Y144, D172, R179, K237, H261, and R264, respectively.

A three-dimensional model of LoxL was computationally constructed based on the sequence and X-ray structure of LoxA. The overall structure of LoxL and a high-magnification view of its active site are presented in Figure 2A and B. The main chains of both Lox structures were well

superimposable, with a root mean square deviation of the atomic Cα position of 0.32 Å. However, the long loop region near the active site of LoxL was different from that of LoxA, primarily due to the 2-residue gap (Fig. 1 and 2B).

```
LoxL  MEKT---YQAGTNEGIVDFINMEDLEIAASQVIPAGGYGYISSGAGDLFTYQENERAFNH 57
LoxA  MNNNDIEYNAPSEIKYIDVVNTYDLEEEASKVVPHGGFNYIAGASGDEWTKRANDRAWKH 60
      *::.   *:* ::   :*.:*  ***  **:*:* **:.**:..:** :* : *:**::*

LoxL  QLIIPHVLRDVELPDTTTHFDEETLTAPIIMAPVAAHGLAHVKAEKASAKGVADFGTIYT 117
LoxA  KLLYPRLAQDVEAPDTSTEILGHKIKAPFIMAPIAAHGLAHTTKEAGTARAVSEFGTIMS 120
      :*: *:: :*** ***:*.:  ..:.**:****:*******.. * .:*:.*::**** :

LoxL  ASSYASCTLEEIREAGGEKAPQWFQFYMSKDNGINLDILEVAKRNGAKAIVLTADATVGG 177
LoxA  ISAYSGATFEEISEG-LNGGPRWFQIYMAKDDQQNRDILDEAKSDGATAIILTADSTVSG 179
       *:*:..*:*** *.  : .*:***:**:**:  * ***: ** :**.**:****:**.*

LoxL  NRETDRRNGFTFPLPMPIVQAYQSG--VGQTMDAVYKSSKQKLSPKDVEFIAAHSDLPVY 235
LoxA  NRDRDVKNKFVYPFGMPIVQRYLRGTAEGMSLNNIYGASKQKISPRDIEEIAGHSGLPVF 239
      **: * :* *.:*: ***** *  *   * ::: :* :****:**:*:* **.**.***:

LoxL  VKGVQSEEDVYRSLESGAGGIWVSNHGGRQLDGGPAAFDSLQYVADAVDKRVPIVFDSGV 295
LoxA  VKGIQHPEDADMAIKRGASGIWVSNHGARQLYEAPGSFDTLPAIAERVNKRVPIVFDSGV 299
      ***:*  **.  ::: **.********.***  .*.:**:*  :*: *:**********

LoxL  RRGQHVFKAIASGADLVAIGRPVIYGLSLGGSTGVRQVFDFFKTELEMVMQLAGTQTVED 355
LoxA  RRGEHVAKALASGADVVALGRPVLFGLALGGWQGAYSVLDYFQKDLTRVMQLTGSQNVED 359
      ***:** **:*****:**:****::**:***  *. .*:*:*:.:*  ****:*:*.***

LoxL  IKKIKLRENRFI    367
LoxA  LKGLDLFDNPYGYEY 374
      :* :.* :* :
```

Fig. 1 Comparison of the amino acid sequences of LoxL (upper: 367 amino acids) and LoxA (lower: 374 amino acids). Identical and similar residues are indicated by asterisks and dots, respectively. Alignment gaps are indicated by dashes. The active site residues are highlighted by gray boxes. The long loop regions near the active sites are surrounded by dashed lines.

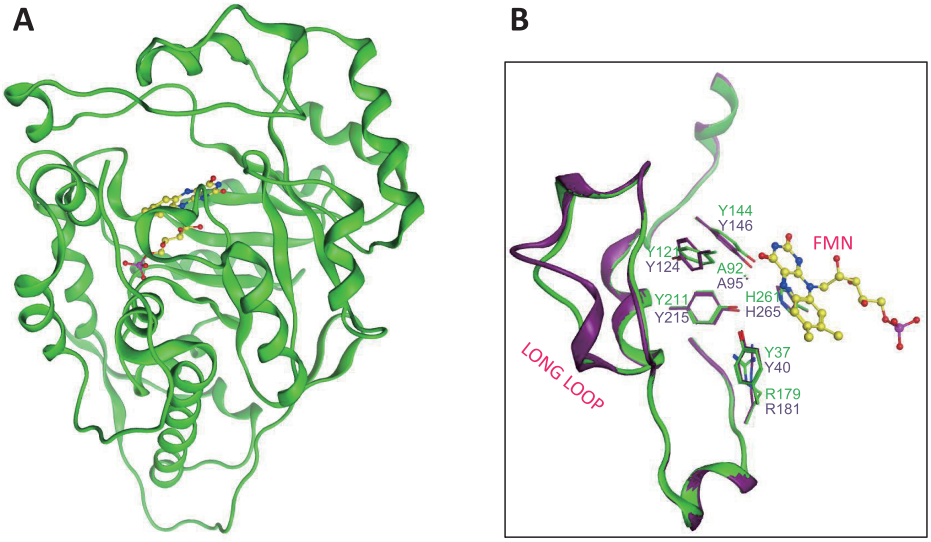

Fig. 2 Model structure of LoxL. (A) Overall structure. The ribbon model was constructed using MOE software. The coenzyme FMN is represented by a ball-and-stick drawing. Carbon, nitrogen, oxygen, and phosphorus atoms are shown in yellow, blue, red, and pink, respectively. (B) High-magnification view of the active site and surrounding region. LoxL (green) is superposed onto the LoxA structure (purple). Side chains of the important amino acid residues are represented as stick structures.

LoxL molecular docking simulations

Molecular docking simulation is a computational method that predicts how ligands interact with a protein. For the purpose of discussing substrate specificity, molecular docking models were constructed for LoxL binding with the substrate L-lactate as well as 3 bulky α-hydroxy acids selected as substrate candidates. A high-magnification view of the active site region of the L-lactate binding model was compared with the active site regions of the L-mandelate, L-glycerate, and L-phenyllactate binding models (Fig. 3).

The binding configuration of LoxL with L-lactate as the substrate-fitting model was consistent with the enzyme's substrate affinity. However, markedly different conditions were observed in substrate-fitting models with the bulky compounds. In particular, notable steric interference was observed between the side chain of Y211 and the benzene ring of L-mandelate. By contrast, steric interference between Y211 and L-glycerate was much weaker than that between Y211 and L-mandelate. The additional hydroxyl group of L-glycerate, moreover, could strengthen the hydrogen bond network in the active site of LoxL. By contrast, no interference between Y211 and L-phenyllactate was observed, because the orientation of the benzene ring differs considerably from that of L-mandelate (Fig. 3). Therefore, it was predicted from these results that the reactivity of LoxL with the bulky α-hydroxy acids increases in order L-mandelate < L-glycerate < L-phenyllactate.

Gene expression and enzyme purification

A Lox activity of 66 U/mL was detected in the crude extract of cultured recombinant E. coli BL21(DE3)(pET-LoxHT). LoxL was then purified to homogeneity as described in the Materials and Methods section. The purified preparation gave a single protein band on SDS-PAGE (Fig. 4) and

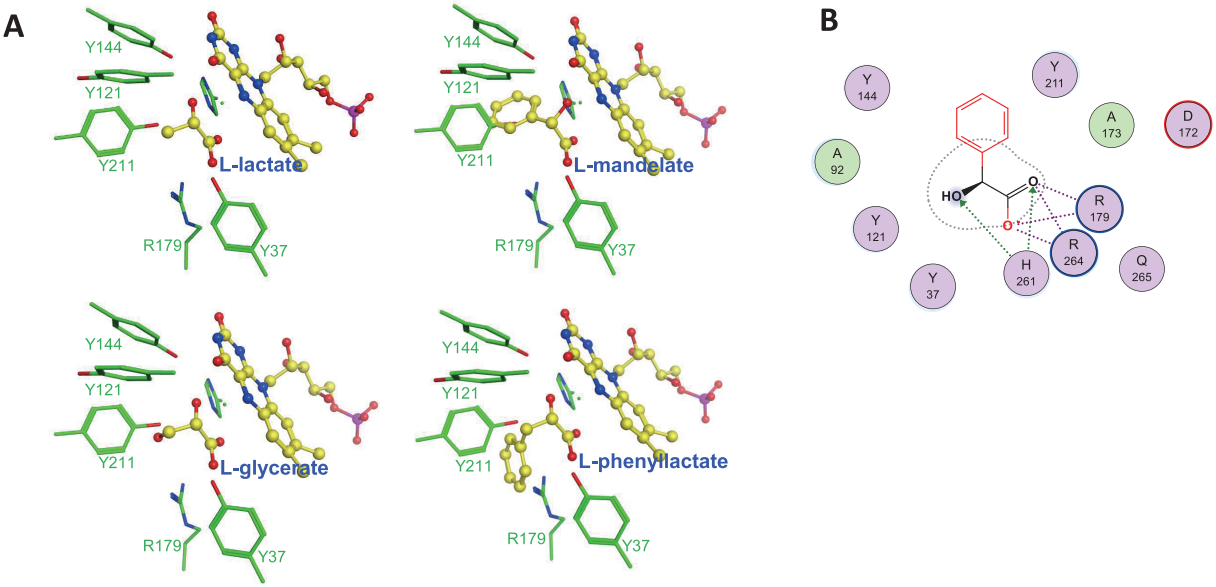

Fig. 3 Docking simulations of LoxL binding to L-lactate, L-mandelate, L-glycerate, and L-phenyllactate. (A) High-magnification views of the active site and each compound. Side chains of the amino acid residues are shown as stick drawings. Each substrate compound and FMN are shown as ball-and-stick drawings. Carbon, nitrogen, oxygen, and phosphorus atoms are shown in yellow, blue, red, and pink, respectively. (B) 2D depiction of the interactions between L-mandelate and LoxL residues. The schematic representation was generated using MOE software. Polar, acidic, basic, and nonpolar residues are shown as different colored disks. Hydrogen bonds are represented as green dotted lines with the arrow denoting the direction of the bond. Electrostatic interactions are represented as purple dotted lines. The solvent exposure of the ligand is expressed as a contoured dotted line, and the solvent exposure of the hydroxyl group is shown as a blue smudge.

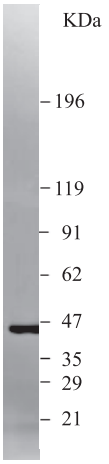

Fig. 4 SDS-PAGE of purified His-tagged LoxL. Molecular weights of markers are shown to the right.

exhibited an absorption spectrum characteristic of a flavoprotein with two peaks at 380 nm and 450 nm. The molecular weight was estimated at 42 kDa by SDS-PAGE, which agreed with that of the monomer His-tagged LoxL calculated from the deduced amino acid sequence and FMN (41.8 kDa).

Enzymatic properties

Details of the substrate specificity of purified LoxL are shown in Table 1. The activity with L-mandelate, DL-glycerate (L-glycerate was commercially unavailable), and L-phenyllactate as substrates was very low as compared with L-lactate as the substrate. Activity against L-mandelate was barely detectable. Although no activity against glycerate was detected in a previous study[1], the assay reagents and conditions in the present study were optimized to increase the sensitivity. The specific activity of LoxL for L-mandelate, DL-glycerate, and L-phenyllactate was 6.6×10^{-5}, 6.6×10^{-3}, and 9.6×10^{-3} of the L-lactate value, respectively. This result accorded with the interpretation based on the structural prediction. As expected, the substrate affinities of LoxL as predicted by comparisons of the active site structures described in this report were demonstrated experimentally.

The K_m value of LoxL for L-lactate was calculated from a Lineweaver-Burk plot as 1.0 mmol/L, which agreed with previous data for the native enzyme[1]. However, the K_m values for the other substrates were too difficult to precisely estimate due to weak activity.

The modeled 3D structure described here could be used in analyses of structure-function relationships and the effects of mutations. The present study provides a reliable basis for identifying sites for directed mutagenesis to deliberately alter the enzyme's activity. Structural predictions of the effects of mutations on substrate specificity and analyses of substrate binding using protein engineering techniques are now in progress.

Conflicts of interest

The authors have no conflicts of interest.

Acknowledgements

We are grateful to Saki Yoshida for her technical assistance.

References

1. Toda A and Nishiya Y: Gene cloning, purification, and characterization of a lactate oxidase from *Lactococcus lactis* subsp. *cremoris* IFO3427. J

Table 1 Substrate specificity of LoxL

Substrate	Specific Activity (U/mg)	Relative Activity
L-lactate	77	1.0
L-mandelate	0.0051	6.6×10^{-5}
DL-glycerate	0.51	6.6×10^{-3}
L-phenyllactate	0.74	9.6×10^{-3}

Ferment Bioeng, 85: 507–510, 1998.
2. Abrar MA, Dong Y, Lee PK, and Kim WS: Bendable electro-chemical lactate sensor printed with silver nano-particles. Scientific Reports, 6: (doi:10.1038/srep30565), 2016.
3. Li SJ, Umena Y, Yorita K, et al.: Crystallographic study on the interaction of L-lactate oxidase with pyruvate at 1.9 Angstrom resolution. Biochem Biophys Res Commun, 358: 1002-1007, 2007.
4. Stoisser T, Rainer D, Leitgeb S, et al.: The ala95-to-gly substitution in *Aerococcus viridans* L-lactate oxidase revisited-structural consequences at the catalytic site and effect on reactivity with O2 and other electron acceptors. FEBS J, 282: 562–578, 2015.
5. Stoisser T, Brunsteiner M, Wilson DK, and Nidetzky B: Conformational flexibility related to enzyme activity: Evidence for a dynamic active-site gatekeeper function of Tyr^{215} in *Aerococcus viridans* lactate oxidase. Scientific Reports, 6: (doi:10.1038/srep27892), 2016.
6. Yorita K: Structure-function relationship of flavoproteins [Jpn]. Seibutsu Butsuri, 42: 66-71, 2002.
7. Umena Y: Reaction mechanism of L-lactate oxidase based on X-ray structural analysis. Osaka University Knowledge Archive (http://hdl.handle.net/11094/23006), 2007.
8. Larkin MA, Blackshields G, Brown NP, et al.: Clustal W and Clustal X version 2.0. Bioinformatics, 23: 2947-2948, 2007.
9. Nishiya Y: Homology modeling and docking study of creatinine deiminase. Int J Anal Bio-Sci, 1: 55-59, 2013.
10. Nishiya Y, Yamamoto M, Takemoto J, et al.: Monomeric sarcosine oxidase exhibiting high substrate affinity and thermostability. Int J Anal Bio-Sci, 4: 55-62, 2016.
11. Nishiya Y, Toda A, and Imanaka T: Gene cluster for creatinine degradation in *Arthrobacter* sp. TE1826. Mol Gen Genet, 257: 581-586, 1998.
12. Inoue H, Nojima H, and Okayama H: High efficiency transformation of *Escherichia coli* with plasmids. Gene, 96: 23-28, 1990.